

Fast algorithm for generating long self-affine profiles

Ingve Simonsen^{1,2,*} and Alex Hansen^{2,3,†}

¹Department of Physics and Astronomy and Institute for Surface and Interface Science, University of California, Irvine, California 92697

²Department of Physics, Theoretical Physics Group, The Norwegian University of Science and Technology,

N-7491 Trondheim, Norway

³International Centre for Condensed Matter Physics, University of Brasília, Caixa Postal 04513, 70919-970 Brasília, Brazil

(Received 7 November 2001; published 1 March 2002)

We introduce a fast algorithm for generating long self-affine profiles. The algorithm, which is based on the fast wavelet transform, is faster than the conventional Fourier filtering algorithm. In addition to increased performance for large systems, the algorithm, named the wavelet filtering algorithm, *a priori* gives rise to profiles for which the long-range correlation extends throughout the entire system independently of the length scale.

DOI: 10.1103/PhysRevE.65.037701

PACS number(s): 02.70.-c, 05.40.-a

With the advent of the computer as a serious research tool, there has been a revolution in the quantitative description of processes and structures that earlier were deemed too complex. Two of the key concepts used for this description are the fractal and its close relative, the self-affine structure [1]. In the early 1980s, much effort was spent in identifying and describing various physical systems having fractal or self-affine structure. As time went by, focus slowly shifted from pure description to asking why such structures would appear? This led to the development of the science of complex growth phenomena. Now, many aspects of these are well understood. However, there are still hosts of interesting but unanswered questions lingering on—see, e.g., Refs. [2–4] for recent reviews. More recently, focus has again begun to shift somewhat, and one sees work dealing with the physical consequences of the presence of fractal or self-affine structures. A concrete example of these three levels of development may be found in the study of fracture surfaces. In the early 1980s, Mandelbrot *et al.* [5] characterized fracture surfaces as self-affine, in the early 1990s attempts were made to understand why fracture surfaces are self-affine [6]. Recently, phenomena such as two-phase flow in fracture joints have been studied [7].

In order to study the physical consequences of the presence of self-affine surfaces, algorithms generating these must be found. There are already several in existence, see, e.g., Feder [1]. However, subtle phenomena require generation of huge surfaces. Two aspects of the algorithms then become important: (i) How self-affine are the surfaces that are generated? and (ii) how fast is the algorithm?

The most popular algorithm used today is the Fourier filtering algorithm (FFA). This algorithm, which has a fast implementation thanks to the fast Fourier transform, consists of generating in the Fourier domain, uncorrelated Gaussian random numbers, which are filtered by a decaying power-law filter of exponent $-2H-1$, where H is the Hurst exponent (to be defined below). By taking advantage of the inverse

fast Fourier transform, self-affine surfaces in real space, with the desirable correlations, are generated.

It has previously been shown [8,9] that the Fourier filtering algorithm has the disadvantage that the self-affine correlations in the limit of large systems only exists over a fraction of the total system size. This is due to aliasing effects. For large enough systems this fraction might be well below 1% (see Fig. 1 for an explicit example). One might overcome the above problem by, e.g., temporarily generating a much larger surface than actually needed, and by using only a small fraction of the total size. This is, however, not a very appealing approach, as the computer time and memory needed easily become too large. Another way of getting around this problem is due to Makse *et al.* [10]. Here the (Fourier-space) filter function is modified by the introduction of a large momentum cutoff through the use of a modified Bessel function in the Fourier transform of the power spectrum. They show that this large momentum cutoff, while

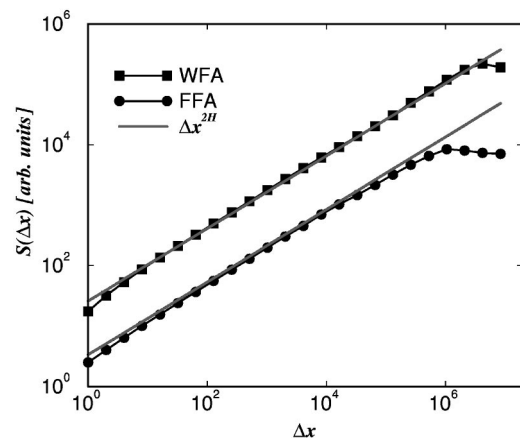


FIG. 1. Second-order structure function $S(\Delta x)$ obtained from one single sample of length $N=2^{25}=33\,554\,432$. The profiles, with prescribed Hurst exponent $H=0.3$, were generated by WFA and FFA, respectively. The solid lines correspond to $S(\Delta x)\sim\Delta x^{2H}$. One observes that the scaling regime of the wavelet generated surface is longer than the one generated by the Fourier method. In particular, the result for the Fourier generated surface exemplifies the claim of Ref. [10] that the scaling regime of FFA generated long surfaces can be as low as 0.1–1 %.

*Email address: Ingve.Simonsen@phys.ntnu.no

†Email address: Alex.Hansen@phys.ntnu.no

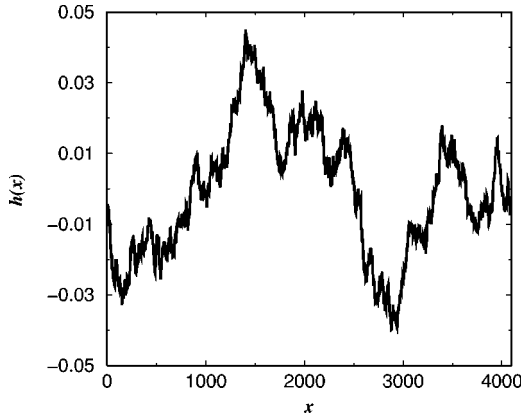


FIG. 2. A self-affine profile $h(x)$ of length $N=4096$ and Hurst exponent $H=0.6$ generated by the wavelet filtering algorithm. The wavelet used in order to generate the profile was the D12 Daubechies wavelet.

irrelevant for the large scale behavior in real space, is essential in order to suppress the aliasing effect and thereby obtaining surfaces with the desired scaling properties over the entire system size.

In this paper we suggest an alternative filtering algorithm based on wavelets, which *a priori*, and without modifications, gives rise to self-affine correlations that extend (up to finite size effects) over the entire system independently of its size (Fig. 1). This algorithm is also computationally cheaper than the traditional (or modified) Fourier filtering algorithm.

For the present discussion we limit ourselves to $(1+1)$ -dimensional surfaces, which we will call *profiles*. A (statistically) self-affine profile $h(x)$ is by definition a structure that remains (statistically) invariant under the following scaling relation:

$$x \rightarrow \lambda x, \quad (1a)$$

$$h \rightarrow \lambda^H h. \quad (1b)$$

Here λ is a real number and H , known as the roughness or Hurst exponent, characterizes this invariance. This exponent is usually in the range from zero to 1. When $H=1/2$, the profile is not correlated. An example of such a profile is the Brownian motion in one dimension. In this case, we interpret time as x and $h(x)$ as the position of the Brownian particle at time x . When $H > 1/2$ the profile is persistent, while when $H < 1/2$ it is antipersistent. We show in Fig. 2 an example of a self-affine profile generated by the algorithm to be presented in this paper.

From the scaling relation (1), one can often, with relatively ease, derive scaling relations for related quantities. In this paper we will later explicitly need the scaling relation for the second-order structure function

$$S(\Delta x) = \langle |h(\Delta x + x) - h(x)|^2 \rangle_x, \quad (2)$$

where $\langle \cdot \rangle_x$ represents the average over the position variable x , and the power spectrum $P(q)$, defined as the Fourier transform of the height-height correlation function, with q being the momentum variable. They scale as [1,3]

$$S(\Delta x) \sim (\Delta x)^{2H}, \quad (3)$$

and

$$P(q) \sim q^{-2H-1}. \quad (4)$$

Below we will make use of these two scaling relations.

The wavelet transform [11–13] of a function $h(x)$ is defined as

$$\mathcal{W}[h](a, b) = \int_{-\infty}^{\infty} dx h(x) \psi_{a,b}^*(x), \quad (5)$$

where $\psi_{a,b}(x)$ is related to the wavelet $\psi(x)$ by

$$\psi_{a,b}(x) = \frac{1}{\sqrt{a}} \psi\left(\frac{x-b}{a}\right). \quad (6)$$

In these expressions a and b denote the scaling and location parameters, respectively.

Recently, the wavelet transform has been used to analyze self-affine profiles [14,15]. In Ref. [15] the authors introduced what they called the average wavelet coefficient function, defined as $W[h](a) = \langle |\mathcal{W}[h](a, b)| \rangle_b$, where $\langle \cdot \rangle_b$ denotes the average over all the location parameters b corresponding to one and the same scale a . For a self-affine function $h(x)$, this quantity should scale as [15]

$$W[h](a) \sim a^{H+1/2}. \quad (7)$$

In much the same way as the Fourier filtering algorithm is used for generating self-affine profiles via the fast Fourier transform, a wavelet based filtering technique can be based on Eq. (7) in combination with the fast wavelet transform. The output of the fast wavelet transform [11–13] is a vector organized as a collection of various levels or hierarchies all of different lengths where each level ℓ is associated with a corresponding scale a_ℓ . The two first components of this vector, also known as level $\ell=0$, are associated to the scaling function. All the other components are “true” wavelet coefficients, such that at level ℓ , corresponding to scale $a_\ell = 2^{-\ell}$ (measured in unit of the profile length), there are $N_\ell = 2^\ell$ coefficients. These coefficients (using our convention) are arranged such that the coefficients of the highest level are found at the end of the vector, and the levels decrease monotonically towards the top of the vector, corresponding to the level $\ell=0$.

Hence, the wavelet based algorithm, which we will be referring to as the *wavelet filtering algorithm* (WFA), consists of the following three steps.

(1) Generate in the wavelet-domain normalized uncorrelated Gaussian numbers $\{\eta_i\}$, with $i=1, 2, \dots, N$ where N is the number of discrete points x_i that together with $h_i = h(x_i)$ constitute the self-affine profile. N is assumed, due to the use of the fast wavelet transform, to be a power of 2.

(2) Filter these random numbers according to

$$w_i = (a_{\ell(i)})^{H+1/2} \frac{\eta_i}{\langle |\eta| \rangle_{\ell(i)}}, \quad i=1, 2, \dots, N$$

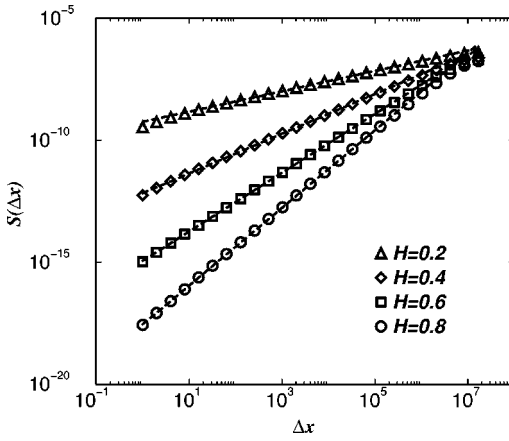


FIG. 3. Average second-order structure function $S(\Delta x)$ obtained by averaging over $N_h=50$ samples (for given H) of the self-affine profile $h(x)$ generated by WFA. All profiles were of length $N=2^{25}=33\,554\,432$. The Hurst exponents used were (from bottom to top) $H=0.8, 0.6, 0.4$, and 0.2 , as indicated in the figure. The dashed lines are the best regression fits corresponding, respectively, to Hurst exponents (from bottom to top) $H=0.80\pm 0.01, 0.60\pm 0.01, 0.41\pm 0.01$, and 0.22 ± 0.02 .

to obtain the wavelet coefficients $\{w_i\}$. Here $a_{\ell(i)}=2^{-\ell(i)}$ represents the scale, at level $\ell(i)$, where $\ell(i)$ is defined as the level corresponding to the location index i of the vector w_i (or η_i). In the above expression the average $\langle |\eta| \rangle_{\ell(i)}$ is understood to be taken over all indices i corresponding to the one and the same level $\ell(i)$.

(3) Perform the inverse fast wavelet transform on $\{w_i\}$, with the (compactly supported) wavelet of your choice, to obtain the (real-space) self-affine profile of predefined Hurst exponent H .

With the wavelet filtering algorithm, good quality self-affine surfaces with predefined Hurst exponent can be generated. In Fig. 2 we show an example of a self-affine surface of Hurst exponent $H=0.6$ and length $N=4096$ generated by the algorithm just outlined. It is worth noting that the above three steps can be modified in order to deal with surfaces in higher dimensions [16]. In this case the speed of the surface generating algorithm becomes very important.

One of the prominent features of the wavelet transform is that the basis functions, the wavelets, are localized in both space and frequency. This has as a consequence, among others, that there is no aliasing, or it is at least heavily suppressed as compared with the Fourier transform. This implies that the wavelet filtering algorithm should automatically result in surfaces that have the desired correlations over the entire length of the profile, and not just a small fraction of it. Hence, independent of the system size, the WFA is capable of generating profiles with well-defined long-range correlations. We will below demonstrate the validity of this claim.

Before turning to the numerical studies of the WFA, we add some remarks regarding the computational efficiency of this algorithm. The most time-consuming part of the WFA is the inverse wavelet transform. To a good approximation, at least for larger system sizes, this time determines the overall computational time of the entire algorithm. The fast wavelet transform needs $O(cN)$ operations, where c is a positive real

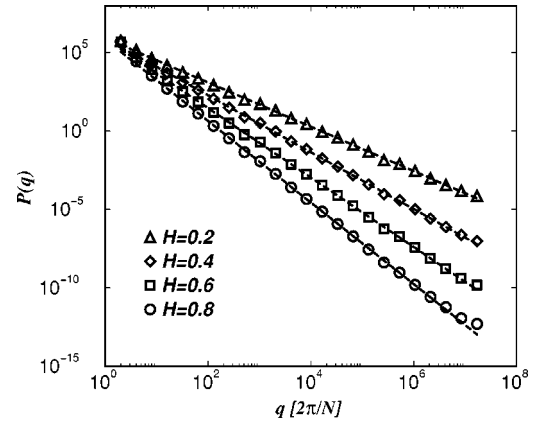


FIG. 4. Average power spectrum $P(q)$ obtained by averaging over $N_h=50$ samples (for given H) of the self-affine profile $h(x)$ generated by WFA. All profiles were of length $N=2^{25}=33\,554\,432$. The Hurst exponents used were (from bottom to top) $H=0.8, 0.6, 0.4$, and 0.2 , as indicated in the figure. The dashed lines are the best regression fits corresponding, respectively, to Hurst exponents (from bottom to top) $H=0.80\pm 0.01, 0.61\pm 0.01, 0.41\pm 0.01$, and 0.20 ± 0.01 .

number whose value depends on the wavelet used [13,17]. Thus, the number of operations needed for generating a surface by WFA is *linear* in the number of points belonging to the profile. In comparison, the Fourier filtering algorithm, whose speed is mainly controlled by the fast Fourier transform, needs $O(N \log_2 N)$ operations to generate a profile. For large system sizes the difference in execution time between WFA and the Fourier filtering algorithm may become significant.

In order to test numerically the predictions made above, we have chosen to study the second-order structure function $S(\Delta x)$ and the power spectrum $P(q)$ of self-affine profiles generated with the wavelet filtering algorithm. The appropriate scaling relations for these two quantities are given by Eqs. (3) and (4). They will provide us with information enabling us to accurately quantify over which length scales the self-affine correlations exist. The numerical experiments, for which the results will be presented shortly, were performed as follows: We generated, by WFA, an ensemble of long self-affine profiles all with the same Hurst exponent H . For each profile the structure function and the power spectrum were calculated, and these were averaged over the ensemble of profiles.

In Fig. 3 we give the numerical results for the second-order structure function obtained as described above. The predefined Hurst exponents, used by the surface generator, were from bottom to top $H=0.8, 0.6, 0.4$, and 0.2 as indicated in the figure. The length of each profile was $N=2^{25}=33\,554\,432$. The number of profiles used in obtaining the averages was $N_h=50$, and the wavelet used was of the Daubechies-type ($D12$) [11–13]. The dashed lines are regression fits to the numerical data. They corresponds (from bottom to top) to Hurst exponents of $H=0.80\pm 0.01, 0.60\pm 0.01, 0.41\pm 0.01$, and 0.22 ± 0.02 , all consistent, within the error bars, with the predefined exponents given above. One easily observes from Fig. 3 that the correlations extend over

all scales except for the largest lags Δx . The reason that the last few large lags do not fit into this general picture is due to finite size effects. We have also undertaken the above analysis for different types of wavelets, taken from the Daubechies family, and for various system sizes, finding no results that are inconsistent with those presented in Fig. 3.

In Fig. 4 we present the average power spectrum obtained using the same surfaces that we used to obtain Fig. 3. The correlations again span most scales. The dashed regression fits lead to the following exponents (from bottom to top): $H = 0.80 \pm 0.01$, 0.61 ± 0.01 , 0.41 ± 0.01 , and 0.20 ± 0.01 , which again are in excellent agreement with the values of the Hurst exponent used for the generation of the underlying profiles.

Figures 3 and 4 indicate that the self-affine correlations span all but the largest scales of the profiles. We stress that this is a generic property of the wavelet filtering algorithm, and no modification of the algorithm is needed in order to handle large system sizes in a satisfactory manner. This is a consequence of the celebrated property of the wavelets being localized *both* in space and frequency.

The calculations of this paper were performed on a SGI/Cray Origin 2000 supercomputer based on the R10000 chip from SGI. On this machine the average CPU time needed for

generating a profile of the length used above ($N = 2^{25}$) was $t_{\text{WFA}} = 45$ s and $t_{\text{FFA}} = 125$ s for the WFA and the traditional (or modified) Fourier filtering algorithm, respectively. Hence the speedup gained by using the wavelet filtering algorithm over the Fourier filter algorithm is close to a factor 3. For system sizes $N \sim 10^3$, we could not observe any significant difference between the two algorithms.

In conclusion, we have introduced a fast and simple algorithm for generating long (or short) self-affine profiles. This algorithm, named the wavelet filtering algorithm, is demonstrated to overcome the problem related to the aliasing effect, which the traditional Fourier filtering algorithm is troubled with. Furthermore, the wavelet based filtering technique outperforms its Fourier-domain counterpart by large margins with respect to computational costs, at least for large system sizes.

I.S. would like to thank the Research Council of Norway and Norsk Hydro ASA for financial support. A.H. thanks H.N. Nazareno and F.A. Oliveira for warm hospitality and the ICCMP for support. This work has received support from the Research Council of Norway (Program for Supercomputing) through a grant of computing time.

-
- [1] J. Feder, *Fractals* (Plenum, New York, 1988).
 - [2] A.L. Barabasi and H.E. Stanley, *Fractal Growth Models* (Cambridge University Press, Cambridge, 1995).
 - [3] P. Meakin, *Phys. Rep.* **235**, 189 (1993).
 - [4] P. Meakin, *Fractals, Scaling, and Growth far from Equilibrium* (Cambridge University Press, Cambridge, 1998).
 - [5] B.B. Mandelbrot, D.E. Passoja, and A.J. Paullay, *Nature (London)* **308**, 721 (1984).
 - [6] E. Bouchaud and J.P. Bouchaud, *Phys. Rev. B* **50**, 17 752 (1994).
 - [7] H. Auradou, K.J. Måløy, J. Schmittbuhl, A. Hansen, and D. Bideau, *Phys. Rev. E* **60**, 7224 (1999).
 - [8] C.K. Peng, S. Havlin, M. Schwartz, and H.E. Stanley, *Phys. Rev. A* **44**, 2239 (1991).
 - [9] S. Prakash, S. Havlin, M. Schwartz, and H.E. Stanley, *Phys. Rev. A* **46**, R1724 (1992).
 - [10] H.A. Makse, S. Havlin, M. Schwartz, and H.E. Stanley, *Phys. Rev. E* **53**, 5445 (1996).
 - [11] W.H. Press, S.A. Teukolsky, W.T. Vetterling and B.P. Flannery, *Numerical Recipes*, 2nd ed. (Cambridge University Press, Cambridge, 1992).
 - [12] I. Daubechies, *Ten Lectures on Wavelets* (SIAM, Philadelphia, 1992).
 - [13] S.G. Mallat, *A Wavelet Tour of Signal Processing* (Academic Press, New York, 1998).
 - [14] A.R. Mehrabi, H. Rassamdana, and M. Sahimi, *Phys. Rev. E* **56**, 712 (1997).
 - [15] I. Simonsen, A. Hansen, and O.M. Nes, *Phys. Rev. E* **58**, 2779 (1998).
 - [16] I. Simonsen (unpublished).
 - [17] S.G. Mallat, *IEEE Trans. Pattern Anal. Mach. Intell.* **11**, 674 (1989).